Supplementary Materials for *Elliptical Insights: Understanding Statistical Methods through Elliptical Geometry*

Michael Friendly
York University

Georges Monette
York University

John Fox
McMaster University

March 24, 2012

Suppplementary materials: Overview

This document describes the supplementary materials included for this paper. One significant component is the material in the Appendix A of this document describing the properties of geometrical and statistical ellipsoids in greater detail than was allowed in the printed version of the paper.

As mentioned in our Discussion (paper: Section 7), one goal of the paper is to make the links between statistical methods, matrix algebra and geometry explicit. Another goal is make our illustrations all statistically and geometrically as nearly exact as possible, and reproducible in standard software (SAS and R). The supplementary materials for these goals are described in Appendix B. We also provide some animated movies of 3D graphs, as described in Appendix C

We understand that all of the materials mentioned below will be provided in some form on the publisher's web site. The same materials, in a form that we can update and possibly extend, will be provided at the first author's web site, `http://datavis.ca/papers/ellipses`.

A Geometrical and statistical ellipsoids

This appendix outlines useful results and properties concerning the representation of geometric and statistical ellipsoids. A number of these can be traced to or have more general descriptions within the abstract formulation of Dempster (1969), (henceforth, $\mathcal{D}$) but casting them in terms of ellipsoids provides a simpler and more easily visualized framework.

A.1 Taxonomy and representation of generalized ellipsoids

Section 2.1 defined a *proper* (origin-centered) ellipsoid in $\mathbb{R}^p$ by $\mathcal{E} := \{\boldsymbol{x} : \boldsymbol{x}^\mathsf{T}\boldsymbol{C}\boldsymbol{x} \leq 1\}$ that is bounded with non-empty interior (call these "fat" ellipsoids). For more general purposes, particularly for statistical applications, it is useful to give ellipsoids a wider definition. To give a complete taxonomy, this wider definition should also include ellipsoids that may be unbounded in some directions in $\mathbb{R}^p$ (an infinite cylinder of ellipsoidal cross-section) and degenerate (singular) ellipsoids that are "flat" in $\mathbb{R}^p$ with empty interior, such as when a 3D ellipsoid has no extent in one dimension (collapsing to an ellipse), or in two dimensions (collapsing to a line). These ideas are made precise below with a definition of the *signature*, $\mathcal{G}(\boldsymbol{C})$, of a generalized ellipsoid.

The motivation for this more general representation is to allow a notation for a set of general ellipsoids to be algebraicly closed under operations (a) image and preimage under a linear transformation and (b) inversion. The goal is to be able to think about, visualize, and *compute* a linear transformation of an ellipsoid with central matrix $\boldsymbol{C}$ or its inverse transformation via an analog of $\boldsymbol{C}^{-1}$, which applies equally to unbounded and/or degenerate ellipsoids. Algebraically, the vector space of $\boldsymbol{C}$ is the *dual* of that of $\boldsymbol{C}^{-1}$ ($\mathcal{D}$ Ch 6) and

vice-versa. Geometrical applications can show how points, lines, and hyperplanes in $\mathbb{R}^p$ are all special cases of ellipsoids. Statistical applications concern the relationship between a predictor data ellipsoid and the corresponding $\boldsymbol{\beta}$ confidence ellipsoid (Section 4.6): The $\boldsymbol{\beta}$ ellipsoid will be unbounded (some linear combinations will have infinite confidence intervals) *iff* the corresponding data ellipsoid is flat, as when $p > n$ or some predictors are collinear.

Defining ellipsoids with $\{\boldsymbol{x} : \boldsymbol{x}^\mathsf{T}\boldsymbol{C}\boldsymbol{x} \leq 1\}$ produces proper ellipsoids for $\boldsymbol{C}$ positive definite and unbounded 'fat' ellipsoids for $\boldsymbol{C}$ positive semi-definite. But it does not produce degenerate (i.e. 'flat') ellipsoids. On the other hand, the representation in Eqn. (3), $\mathcal{E} := \boldsymbol{A}\mathcal{S}$, with $\mathcal{S}$ the unit sphere, produces proper ellipsoids when $\boldsymbol{C} = \left(\boldsymbol{A}^\mathsf{T}\boldsymbol{A}\right)^{-1}$ where $\boldsymbol{A}$ is a non-singular $p \times p$ matrix and degenerate ellipsoids when $\boldsymbol{A}$ is a singular, but does not produce unbounded ellipsoids.

One representation that works for all of fat or flat *and* bounded or unbounded ellipsoids can be based on an SVD representation $\boldsymbol{A} = \boldsymbol{U}\boldsymbol{\Delta}\boldsymbol{V}^\mathsf{T}$, with

$$\mathcal{E} := \boldsymbol{U}(\boldsymbol{\Delta}\mathcal{S}) \ , \tag{A.1}$$

where $\boldsymbol{U}$ is orthogonal and $\boldsymbol{\Delta}$ is diagonal with non-negative reals or infinity.[1] The 'inverse' of an ellipsoid $\mathcal{E}$ is then simply $\boldsymbol{U}(\boldsymbol{\Delta}^{-1}\mathcal{S})$. The connection with traditional representations is that, if $\boldsymbol{\Delta}$ is finite, $\boldsymbol{A} = \boldsymbol{U}\boldsymbol{\Delta}\boldsymbol{V}^\mathsf{T}$ where $\boldsymbol{V}$ can be any orthogonal matrix and if $\boldsymbol{\Delta}^{-1}$ is finite, $\boldsymbol{C} = \boldsymbol{U}\boldsymbol{\Delta}^{-2}\boldsymbol{U}^\mathsf{T}$.

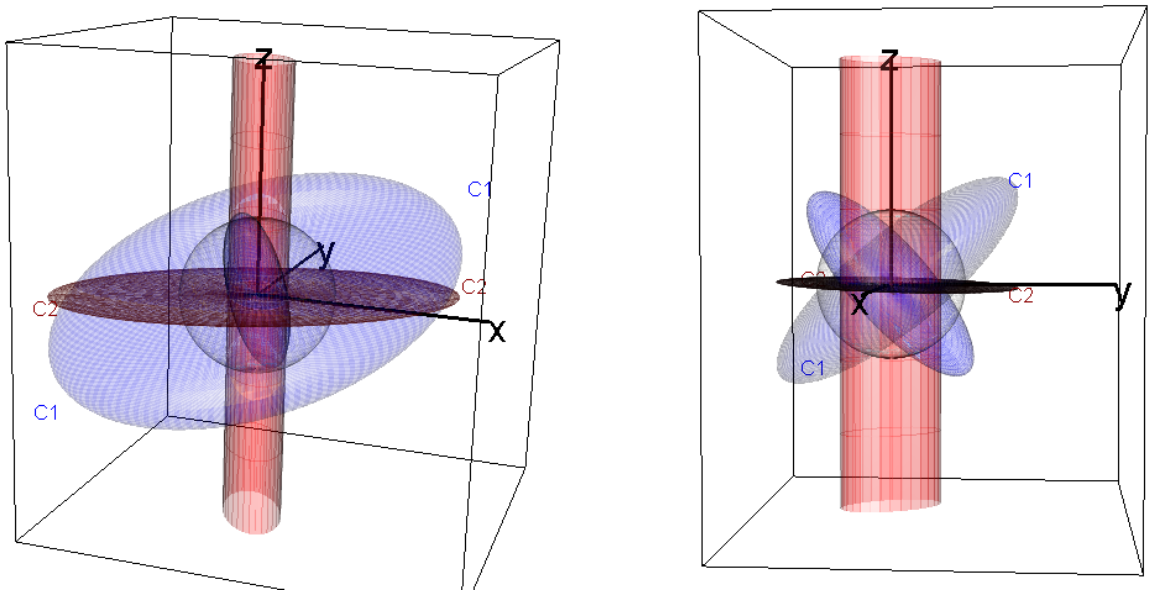

Figure A.1: Two views of an example of generalized ellipsoids. $\boldsymbol{C}_1$ (blue) determines a proper, fat ellipsoid; its inverse $\boldsymbol{C}_1^{-1}$ also generates a proper ellipsoid. $\boldsymbol{C}_2$ (red) determines an improper, flat ellipsoid, whose inverse $\boldsymbol{C}_2^{-1}$ is an unbounded cylinder of elliptical cross section. The scale of these images is defined by a unit sphere (gray). The right panel shows a view illustrating the orthogonality of each $\boldsymbol{C}$ and its dual, $\boldsymbol{C}^{-1}$.

The $\boldsymbol{U}(\boldsymbol{\Delta}\mathcal{S})$ representation also allow us to characterize any such generalized ellipsoid in $\mathbb{R}^p$ by its *signature*,

$$\mathcal{G}(\boldsymbol{C}) = [\#(\delta_i > 0), \#(\delta_i = 0), \#(\delta_i = \infty)] \quad \text{with} \quad \sum \mathcal{G}(\boldsymbol{C}) = p \ , \tag{A.2}$$

a 3-vector containing the number of positive, zero and infinite singular values. For example, in $\mathbb{R}^3$, any proper ellipsoid has the signature $\mathcal{G}(\boldsymbol{C}) = (3, 0, 0)$, a flat, 2D ellipsoid has $\mathcal{G}(\boldsymbol{C}) = (2, 1, 0)$, a flat, 1D ellipsoid (a

[1] Note that the parentheses in this notation are obligatory: $\boldsymbol{\Delta}$ as defined transforms the unit sphere, which is then transformed by $\boldsymbol{U}$. $\boldsymbol{V}^\mathsf{T}$, also orthogonal, plays no role in this representation, because an orthogonal transformation of $\mathcal{S}$ is still a unit sphere.

line) has $\mathcal{G}(\boldsymbol{C}) = (1, 2, 0)$. Unbounded examples include an infinite flat plane, with $\mathcal{G}(\boldsymbol{C}) = (0, 1, 2)$, and an infinite cylinder of elliptical cross-section, with $\mathcal{G}(\boldsymbol{C}) = (2, 0, 1)$.

Figure A.1 illustrates these ideas, using two generating matrices, $\boldsymbol{C}_1$ and $\boldsymbol{C}_2$ in this more general representation,

$$\boldsymbol{C}_1 = \begin{bmatrix} 6 & 2 & 1 \\ 2 & 3 & 2 \\ 1 & 2 & 2 \end{bmatrix} \quad , \qquad \boldsymbol{C}_2 = \begin{bmatrix} 6 & 2 & 0 \\ 2 & 3 & 0 \\ 0 & 0 & 0 \end{bmatrix}$$

where $\boldsymbol{C}_1$ generates a proper ellipsoid and $\boldsymbol{C}_2$ generates an improper, flat ellipsoid. $\boldsymbol{C}_1$ and its dual, $\boldsymbol{C}_1^{-1}$ both have signatures $(3, 0, 0)$. $\boldsymbol{C}_2$ has the signature $(2, 1, 0)$, while its inverse (dual) has the signature $(2, 0, 1)$. These varieties of ellipsoids are more easily seen in the 3D movies included in the online supplements.

A.2 Properties of geometric ellipsoids

- Translation: An ellipsoid centered at $\boldsymbol{x}_0$ has the definition $\mathcal{E} := \{\boldsymbol{x} : (\boldsymbol{x} - \boldsymbol{x}_0)^\mathsf{T} \boldsymbol{C} (\boldsymbol{x} - \boldsymbol{x}_0) = 1\}$ or $\mathcal{E} := \boldsymbol{x}_0 \oplus \boldsymbol{A}\mathcal{S}$ in the notation of Section 2.2.

- Orthogonality: If $\boldsymbol{C}$ is diagonal, the origin-centered ellipsoid has its axes aligned with the coordinate axes, and has the equation

$$\boldsymbol{x}^\mathsf{T} \boldsymbol{C} \boldsymbol{x} = c_{11} x_1^2 + c_{22} x_2^2 + \cdots + c_{pp} x_p^2 = 1 \ , \tag{A.3}$$

  where $1/\sqrt{c_{ii}} = c_{ii}^{-1/2}$ are the radii (semi-diameter lengths) along the coordinate axes.

- Area and volume: In two dimensions, the area of the axis-aligned ellipse is $\pi(c_{11}c_{22})^{-1/2}$. For $p = 3$, the volume is $\frac{4}{3}\pi(c_{11}c_{22}c_{33})^{-1/2}$. In the general case, the hypervolume of the ellipsoid is proportional to $|\boldsymbol{C}|^{-1/2} = ||\boldsymbol{A}||$ and is given by $\pi^{p/2}\det(\boldsymbol{C})^{-1/2} / \left[\Gamma\left(\frac{p}{2} + 1\right)\right]$, where the first two factors are familiar as the normalizing constant of the multivariate normal density function.

- Principal axes: In general, the eigenvectors, $\boldsymbol{v_i}, i = 1, \ldots, p$, of $\boldsymbol{C}$ define the principal axes of the ellipsoid and the inverse of the square roots of the ordered eigenvalues, $\lambda_1 > \lambda_2 \ldots, \lambda_p$, are the principal radii. Eigenvectors belonging to eigenvalues that are 0 are directions in which the ellipsoid is unbounded. With $\mathcal{E} = \boldsymbol{A}\mathcal{S}$, we consider the singular-value decomposition $\boldsymbol{A} = \boldsymbol{U}\boldsymbol{D}\boldsymbol{V}^\mathsf{T}$, with $\boldsymbol{U}$ and $\boldsymbol{V}$ orthogonal matrices and $\boldsymbol{D}$ a diagonal non-negative matrix with the same dimension as $\boldsymbol{A}$. The column vectors of $\boldsymbol{U}$, called the left singular vectors, correspond to the eigenvectors of $\boldsymbol{C}$ in the case of a proper ellipsoid. The positive diagonal elements of $\boldsymbol{D}$, $d_1 > d_2 > ... > d_p > 0$, are the principal radii of the ellipse with $d_i = 1/\sqrt{\lambda_i}$. In the singular case, the left singular vectors form a set of principal axes for the flattened ellipsoid.[2]

- Inverse: When $\boldsymbol{C}$ is positive definite, the eigenvectors of $\boldsymbol{C}$ and $\boldsymbol{C}^{-1}$ are identical, while the eigenvalues of $\boldsymbol{C}^{-1}$ are $1/\lambda_i$. It follows that the ellipsoid for $\boldsymbol{C}^{-1}$ has the same axes as that of $\boldsymbol{C}$, but with inversely proportional radii. In $\mathbb{R}^2$, the ellipsoid for $\boldsymbol{C}^{-1}$ is, with rescaling, a 90° rotation of the ellipsoid for $\boldsymbol{C}$, as illustrated in Figure A.2.

- Generalized inverse: A definition for an inverse ellipsoid that is equivalent in the case of proper ellipsoids,

$$\mathcal{E}^{-1} := \{\boldsymbol{y} : |\boldsymbol{x}^\mathsf{T}\boldsymbol{y}| \leq 1 \ , \quad \forall \boldsymbol{x} \in \mathcal{E}\} \ , \tag{A.4}$$

  generalizes to all ellipsoids. The inverse of a singular ellipsoid is an improper ellipsoid and vice versa.

[2]Corresponding left singular vectors and eigenvectors are not necessarily equal but sets that belong to the same eigenvalue/singular value span the same space.

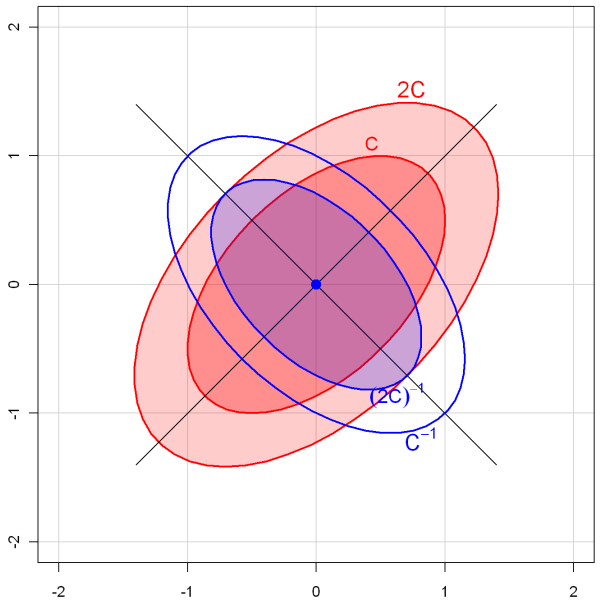

Figure A.2: Some properties of geometric ellipsoids. Principal axes of an ellipsoid are given by the eigenvectors of $\boldsymbol{C}$, with radii $1/\sqrt{\lambda_i}$. For an ellipsoid defined by Eqn. (1), the comparable ellipsoid for $2\boldsymbol{C}$ has radii multiplied by $1/\sqrt{2}$. The ellipsoid for $\boldsymbol{C}^{-1}$ has the same principal axes, but with radii $\sqrt{\lambda_i}$, making it small in the directions where $\boldsymbol{C}$ is large and vice-versa.

- Dimensionality: The ellipsoid is bounded if $\boldsymbol{C}$ is positive definite (all $\lambda_i > 0$). Each $\lambda_i = 0$ increases the dimension of the space along which the ellipsoid is unbounded by one. For example, with $p = 3$, $\lambda_3 = 0$ gives a cylinder with an elliptical cross-section in 3-space, and $\lambda_2 = \lambda_3 = 0$ gives an infinite slab with thickness $2\sqrt{\lambda_1}$. With $\mathcal{E} = \boldsymbol{A}\mathcal{S}$, the dimension of the ellipsoid is equal to the number of positive singular values of $\boldsymbol{A}$.

- Projections: The projection of a p dimensional ellisoid into any subspace is $\boldsymbol{P}\mathcal{E}$, where $\boldsymbol{P}$ is an idempotent $p \times p$ (projection) matrix, i.e., $\boldsymbol{P}\boldsymbol{P} = \boldsymbol{P}^2 = \boldsymbol{P}$. For example, in $\mathbb{R}^2$ and $\mathbb{R}^3$, the matrices

$$\boldsymbol{P}_2 = \begin{bmatrix} 1 & 1 \\ 0 & 0 \end{bmatrix} , \qquad \boldsymbol{P}_3 = \begin{bmatrix} 1 & 0 & 0 \\ 0 & 1 & 0 \\ 0 & 0 & 0 \end{bmatrix}$$

  project, respectively, an ellipse onto the line $x_1 = x_2$, and an ellipsoid into the (x_1, x_2) plane. If $\boldsymbol{P}$ is symmetric, then $\boldsymbol{P}$ is the matrix of an orthogonal projection, and it is easy to visualize $\boldsymbol{P}\mathcal{E}$ as the shadow of $\mathcal{E}$ cast perpendicularly onto $\mathrm{span}(\boldsymbol{P})$. Generally, $\boldsymbol{P}\mathcal{E}$ is the shadow of $\mathcal{E}$ onto $\mathrm{span}(\boldsymbol{P})$ along the null space of $\boldsymbol{P}$.

- Linear transformations: A linear transformation of an ellipsoid is an ellipsoid, and the pre-image of an ellipsoid under a linear transformation is an ellipsoid. A non-singular linear transformation maps a proper ellipsoid into a proper ellipsoid.

- Slopes and tangents: The slopes of the ellipsoidal surface in the directions of the coordinate axes are given by $\partial/\partial\boldsymbol{x}\ (\boldsymbol{x}^\mathsf{T}\boldsymbol{C}\boldsymbol{x}) = 2\boldsymbol{C}\boldsymbol{x}$. From this, it follows that the tangent hyperplane to the unit ellipsoidal surface at the point $\boldsymbol{x}_\alpha$, where $\boldsymbol{x}_\alpha^\mathsf{T}\ \partial/\partial\boldsymbol{x}(\boldsymbol{x}^\mathsf{T}\boldsymbol{C}\boldsymbol{x}) = 0$, has the equation $\boldsymbol{x}_\alpha^\mathsf{T}\boldsymbol{C}\boldsymbol{x} = 1$.

A.3 Conjugate axes and inner-product spaces

For any non-singular $\boldsymbol{A}$ in Eqn. (5) that generates an ellipsoid, the columns of $\boldsymbol{A} = [\boldsymbol{a}_1, \boldsymbol{a}_2, \cdots, \boldsymbol{a}_p]$ form a set of "conjugate axes" of the ellipse. (Two diameters are conjugate *iff* the tangent line at the endpoint of one diameter is parallel to the other diameter.) Each vector $\boldsymbol{a}_i$ lies on the ellipse, and the tangent hyperplane at that point is parallel to the span of all the other column vectors of $\boldsymbol{A}$. For $p = 2$ this result is illustrated in

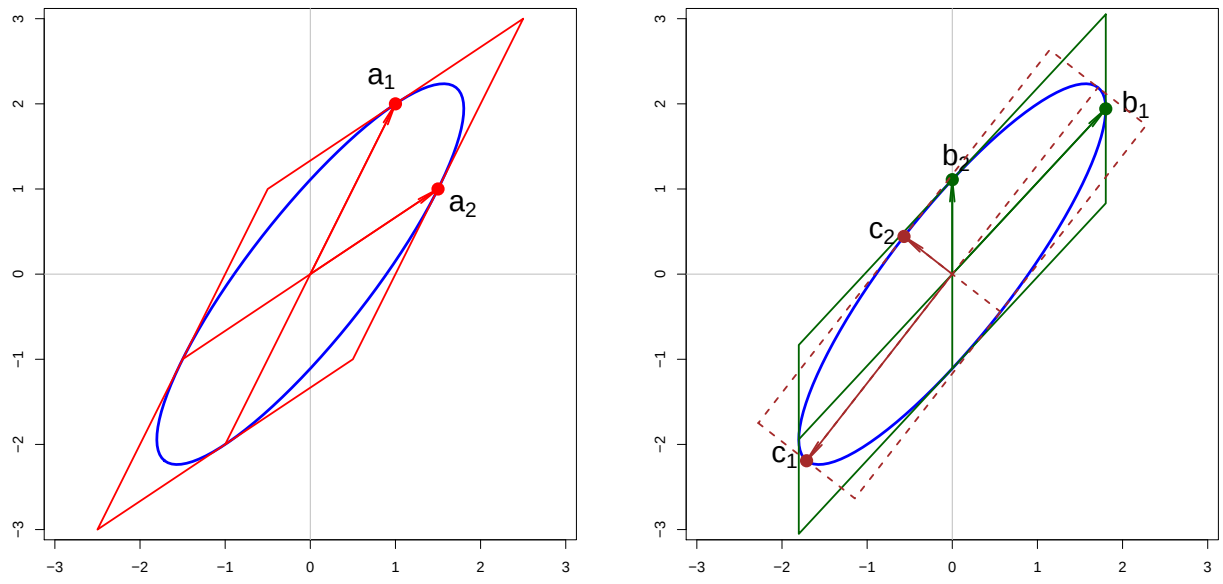

Figure A.3: Conjugate axes of an ellipsoid with various factorizations of $\boldsymbol{W}$ and corresponding basis vectors. The conjugate vectors lie on the ellipsoid, and their tangents can be extended to form a parallelogram framing it. Left: for an arbitrary factorization, given in Eqn. (A.5). Right: for the Choleski factorization (solid, green, b_1, b_2) and the principal component factorization (dashed, brown, c_1, c_2).

Figure A.3 (left) in which

$$\boldsymbol{A} = \begin{bmatrix} \boldsymbol{a}_1 & \boldsymbol{a}_2 \end{bmatrix} = \begin{bmatrix} 1 & 1.5 \\ 2 & 1 \end{bmatrix} \;\Rightarrow\; \boldsymbol{W} = \boldsymbol{A}\boldsymbol{A}^{\mathsf{T}} = \begin{bmatrix} 3.25 & 3.5 \\ 3.5 & 5 \end{bmatrix} \;. \tag{A.5}$$

Consider the inner-product space with inner product matrix $\boldsymbol{W}^{-1} = \begin{bmatrix} 1.25 & -0.875 \\ -0.875 & 0.8125 \end{bmatrix}$ and inner product

$$\langle \boldsymbol{x}, \boldsymbol{y} \rangle = \boldsymbol{x}'\boldsymbol{W}^{-1}\boldsymbol{y} \;.$$

Because $\boldsymbol{A}^{\mathsf{T}}\boldsymbol{W}^{-1}\boldsymbol{A} = \boldsymbol{A}^{\mathsf{T}}\left(\boldsymbol{A}\boldsymbol{A}^{\mathsf{T}}\right)^{-1}\boldsymbol{A} = \boldsymbol{A}^{\mathsf{T}}(\boldsymbol{A}^{\mathsf{T}})^{-1}\boldsymbol{A}^{-1}\boldsymbol{A} = \boldsymbol{I}$, we see that $\boldsymbol{a}_1$ and $\boldsymbol{a}_2$ are orthogonal unit vectors (in fact, an orthonormal basis) in this inner product:

$$\begin{aligned} \langle \boldsymbol{a}_i, \boldsymbol{a}_i \rangle &= \boldsymbol{a}_i^{\mathsf{T}}\boldsymbol{W}^{-1}\boldsymbol{a}_i = 1 \\ \langle \boldsymbol{a}_1, \boldsymbol{a}_2 \rangle &= \boldsymbol{a}_1'\boldsymbol{W}^{-1}\boldsymbol{a}_2 = 0 \;. \end{aligned}$$

Now, if $\boldsymbol{W} = \boldsymbol{B}\boldsymbol{B}^{\mathsf{T}}$ is any other factorization of $\boldsymbol{W}$, then the columns of $\boldsymbol{B}$ have the same properties as the columns of $\boldsymbol{A}$. Particular factorizations yield interesting and statistically useful sets of conjugate axes. The illustration in Figure A.3 (right) shows two such cases with special properties: In the Choleski factorization (shown solid in green), where $\boldsymbol{B}$ is lower triangular, the last conjugate axis, $\boldsymbol{b}_2$, is aligned with

the coordinate axis $\boldsymbol{x}_2$. Each previous axis ($\boldsymbol{b}_1$, here) is the orthogonal complement to all later axes in the inner-product space of $\boldsymbol{W}^{-1}$. The Choleski factorization is unique in this respect, subject to a permutation of the rows and columns of $\boldsymbol{W}$. The subspace $\{c_1\boldsymbol{b}_1 + ... + c_{p-1}\boldsymbol{b}_{p-1}, c_i \in \mathbb{R}\}$, is the plane of the regression of the last variable on the others, a fact that generalizes naturally to ellipsoids that are not necessarily centerered at the origin.

In the principal-component (PC) factorization (shown dashed in brown) $\boldsymbol{W} = \boldsymbol{C}\boldsymbol{C}^\mathsf{T}$, where $\boldsymbol{C} = \boldsymbol{\Gamma}\boldsymbol{\Lambda}^{1/2}$ and hence $\boldsymbol{W} = \boldsymbol{\Gamma}\boldsymbol{\Lambda}\boldsymbol{\Gamma}'$ is the spectral decomposition of $\boldsymbol{W}$. Here, the ellipse axes are orthogonal in the space of the ellipse (so the bounding tangent parallelogram is a rectangle) *as well as* in the inner-product space of $\boldsymbol{W}^{-1}$. The PC factorization is unique in this respect (up to reflections of the axis vectors).

As illustrated in Figure A.3, each pair of conjugate axes has a corresponding bounding tangent parallelogram. It can be shown that all such parallelograms have the same area and equal sums of squares of the lengths of their diameters.

A.4 Ellipsoids in a generalized metric space

In Appendix A.3, we considered the positive semi-definite matrix $\boldsymbol{W}$ and corresponding ellipsoid to be referred to a Euclidean space, perhaps with different basis vectors. We showed that various measures of the "size" of the ellipsoid could be defined in terms of functions of the eigenvalues λ_i of $\boldsymbol{W}$.

We now consider the generalized case of an analogous $p \times p$ positive semi-definite symmetric matrix $\boldsymbol{H}$, but where measures of length, distance, and angles are referred to a metric defined by a positive-definite symmetric matrix $\boldsymbol{E}$. As is well known, the generalized eigenvalue problem is to find the scalars λ_i and vectors $\boldsymbol{v}_i, i = 1, 2, \ldots p$, such that $\boldsymbol{H}\boldsymbol{v} = \lambda\boldsymbol{E}\boldsymbol{v}$, that is, the roots of $\det(\boldsymbol{H} - \lambda\boldsymbol{E}) = 0$.

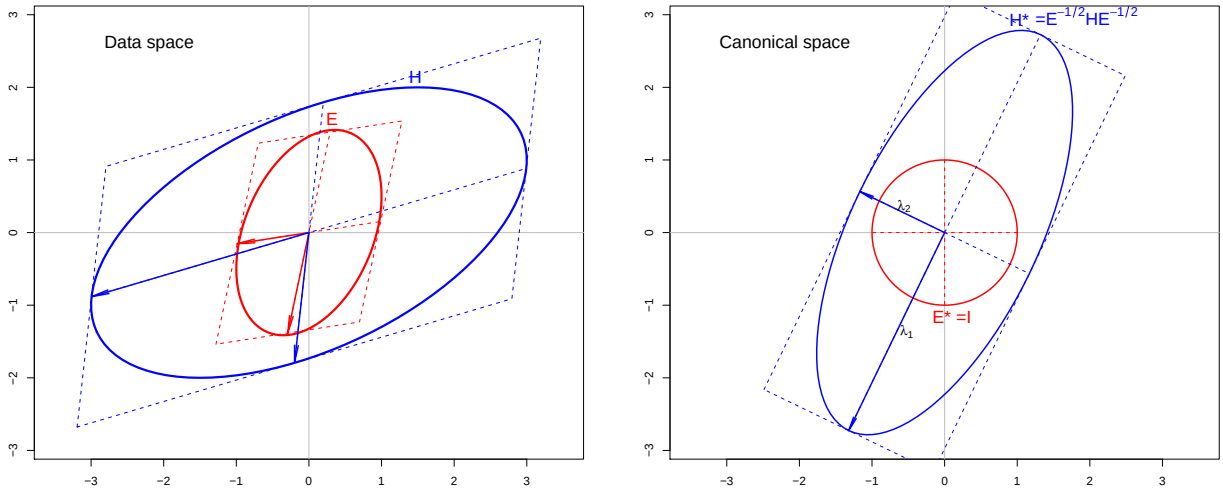

Figure A.4: Left: Ellipses for $\boldsymbol{H}$ and $\boldsymbol{E}$ in Euclidean "data space." Right: Ellipses for $\boldsymbol{H}^\star$ and $\boldsymbol{E}^\star$ in the transformed "canonical space," with the eigenvectors of $\boldsymbol{H}$ relative to $\boldsymbol{E}$ shown as blue arrows, whose radii are the corresponding eigenvalues, λ_1, λ_2.

For such $\boldsymbol{H}$ and $\boldsymbol{E}$, we can always find a factor $\boldsymbol{A}$ of $\boldsymbol{E}$, so that $\boldsymbol{E} = \boldsymbol{A}\boldsymbol{A}^\mathsf{T}$, whose colums will be conjugate directions for $\boldsymbol{E}$ and whose rows will also be conjugate directions for $\boldsymbol{H}$, in that $\boldsymbol{H} = \boldsymbol{A}^\mathsf{T}\boldsymbol{D}\boldsymbol{A}$, where $\boldsymbol{D}$ is diagonal. Geometrically, this means that there exists a unique pair of bounding parallelograms for the $\boldsymbol{H}$ and $\boldsymbol{E}$ ellipsoids whose corresponding sides are parallel. A linear transformation of $\boldsymbol{E}$ and $\boldsymbol{H}$ that transforms the parallelogram for $\boldsymbol{E}$ to a square (or cuboid), and hence $\boldsymbol{E}$ to a sphere (or spheroid), generates an equivalent view in what we describe below as canonical space.

In statistical applications (e.g., MANOVA, canonical correlation), the generalized eigenvalue problem is transformed to an ordinary eigenvalue problem by considering the following equivalent forms with the same λ_i, $\boldsymbol{v}_i$,

$$\begin{aligned} (\boldsymbol{H} - \lambda \boldsymbol{E})\boldsymbol{v} &= \mathbf{0} \\ \Rightarrow (\boldsymbol{H}\,\boldsymbol{E}^{-1} - \lambda \boldsymbol{I})\boldsymbol{v} &= \mathbf{0} \\ \Rightarrow (\boldsymbol{E}^{-1/2}\,\boldsymbol{H}\,\boldsymbol{E}^{-1/2} - \lambda \boldsymbol{I})\boldsymbol{v} &= \mathbf{0}\ , \end{aligned}$$

where the last form gives a symmetric matrix, $\boldsymbol{H}^\star = \boldsymbol{E}^{-1/2}\,\boldsymbol{H}\,\boldsymbol{E}^{-1/2}$. Using the square root of $\boldsymbol{E}$ defined by the principal-component factorization $\boldsymbol{E}^{1/2} = \boldsymbol{\Gamma}\boldsymbol{\Lambda}^{1/2}$ produces the ellipsoid $\boldsymbol{H}^\star$, the orthogonal axes of which correspond to the $\boldsymbol{v}_i$, whose squared radii are the corresponding eigenvalues λ_i. This can be seen geometrically as a rotation of "data space" to an orientation defined by the principal axes of $\boldsymbol{E}$, followed by a re-scaling, so that the $\boldsymbol{E}$ ellipsoid becomes the unit spheroid. In this transformed space ("canonical space"), functions of the the squared radii λ_i of the axes of $\boldsymbol{H}^\star$ give direct measures of the "size" of $\boldsymbol{H}$ relative to $\boldsymbol{E}$. The orientation of the eigenvectors $\boldsymbol{v}_i$ can be related to the (orthogonal) linear combinations of the data variables that are successively largest in the metric of $\boldsymbol{E}$.

To illustrate, Figure A.4 (left) shows the ellipses generated by

$$\boldsymbol{H} = \begin{bmatrix} 9 & 3 \\ 3 & 4 \end{bmatrix} \quad \text{and} \quad \boldsymbol{E} = \begin{bmatrix} 1 & 0.5 \\ 0.5 & 2 \end{bmatrix}$$

together with their conjugate axes. For $\boldsymbol{E}$, the conjugate axes are defined by the columns of the right factor, $\boldsymbol{A}^\mathsf{T}$, in $\boldsymbol{E} = \boldsymbol{A}\boldsymbol{A}^\mathsf{T}$; for $\boldsymbol{H}$, the conjugate axes are defined by the columns of $\boldsymbol{A}$. The transformation to $\boldsymbol{H}^\star = \boldsymbol{E}^{-1/2}\,\boldsymbol{H}\,\boldsymbol{E}^{-1/2}$ is shown in the right panel of Figure A.4. In this "canonical space," angles and lengths have the orginary interpretation of Euclidean space, so the size of $\boldsymbol{H}^\star$ can be interpreted directly in terms of functions of the radii $\sqrt{\lambda_1}$ and $\sqrt{\lambda_2}$.

B SAS and R code for figures

We provide the source code used to generate all of the figures with this supplement in the file `ellipses-suppfiles.zip`. It should be noted that these illustrations were developed over a considerable period of time, using a collection of general SAS macro programs and R packages by the authors and others (listed below). It often happened that these software tools were not sufficiently general or capable for our purposes. In many cases the SAS macros and R packages were extended (or a new package was written, e.g., the **genridge** package (Friendly, 2011, 2012) for the material on ridge trace plots in Section 6.3.1) to make these analyses and figures easier to do in the future. However, once we enhanced the SAS macros or R packages, we did not often go back and re-do the figures using the revised tools.

B.1 Macros and R packages

The SAS programs use a collection of SAS macros, available from the website `http://datavis.ca/sasmac/`. See `http://datavis.ca/books/sssg/usage.html` for installation and usage notes.

The following R packages beyond those standardly installed with R itself are available from any CRAN mirror site, e.g., `http://cran.us.r-project.org`: **candisc**, **car**, **ellipse**, **heplots**, **mvmeta**, **sfsmisc**. Two other package, still under development by the authors are available from the R-Forge server, `http://r-forge.r-project.org`: **p3d** (Monette *et al.*, 2011) and **spida** (Monette, 2011).

B.2 Visual directory for figures

SAS and R source files are containted in the directories `SAS/` and `R/` respectively. The table below shows thumbnails of the figures together with the name of the SAS or R source file.

Paper

Fig. 2
SAS/galton-reg3.sas

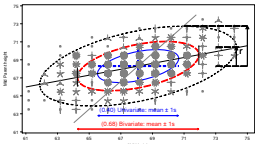

Fig. 3
SAS/scatirisd.sas

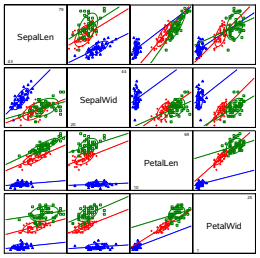

Fig. 4
R/ellipses-demo.R

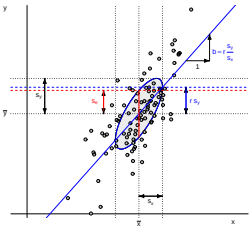

Fig. 5
R/vis-reg-prestige.R

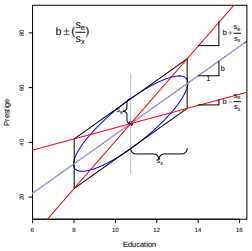

Fig. 6
SAS/contiris.sas

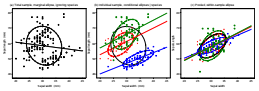

Fig. 7
R/between-within.R

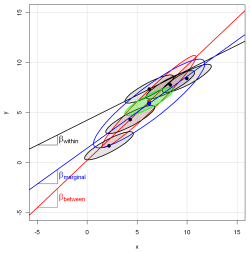

Fig. 8
R/between-within.R

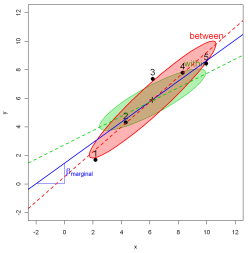

Fig. 9
SAS/levdemo2.sas

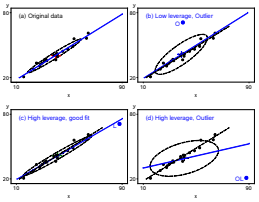

Fig. 11
R/vis-reg-coffee1.R

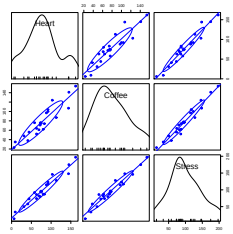

Fig. 12
R/vis-reg-coffee1.R

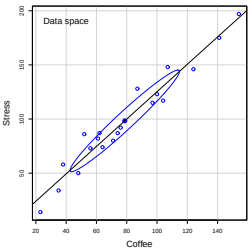

Fig. 13
R/vis-reg-coffee1.R

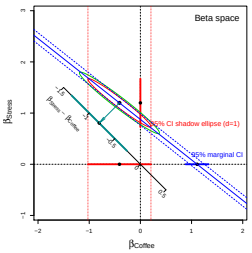

Fig. 14
R/coffee-stress.R

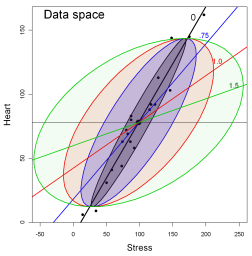

Fig. 15
R/coffee-measerr.R

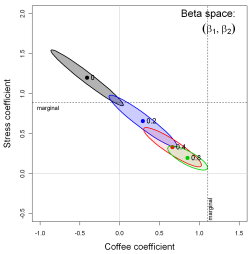

Fig. 16
R/coffee-avPlots.R

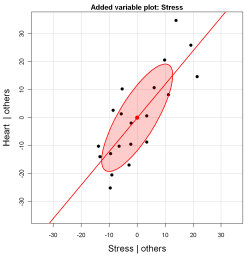

Fig. 17
R/coffee-av3D.R

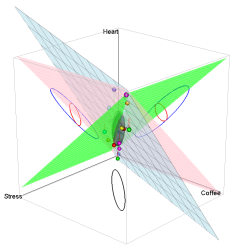

Fig. 18
R/coffee-avPlots.R

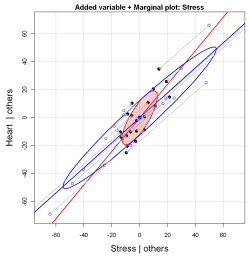

Fig. 19
R/mtests.R

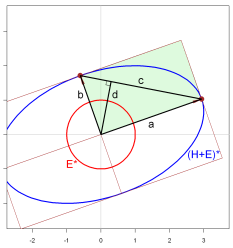

Fig. 20
SAS/heplot3a.sas

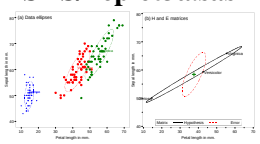

Fig. 21
R/HE-contrasts-iris.R

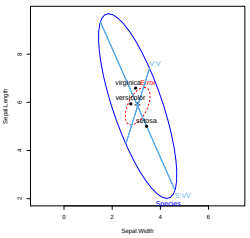

Fig. 22
R/HE-can-iris.R

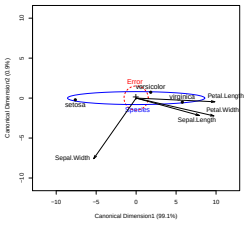

Fig. 23	Fig. 24	Fig. 25	Fig. 26
R/kiss-demo.R	**R/kiss-demo2.R**	**R/ridge-demo.R**	**R/ridge2.R**
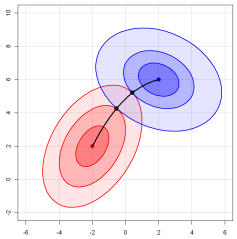	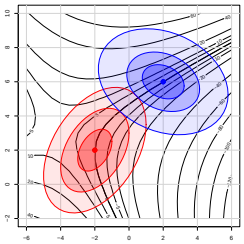	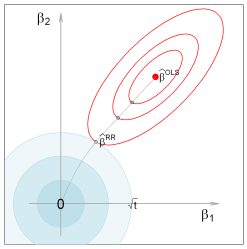	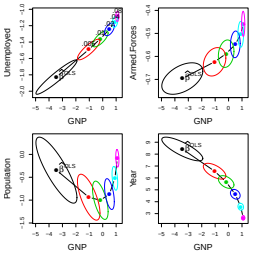

Fig. 27	Fig. 28	Fig. 29
SAS/hsbmix4.sas	**SAS/hsbmix4.sas**	**R/mvmeta2.R**
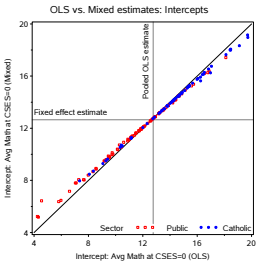	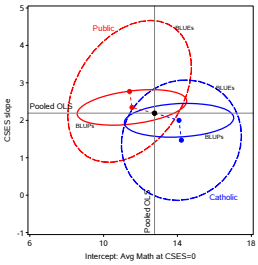	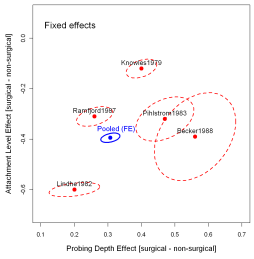

Appendix

Fig. A.1	Fig. A.2	Fig. A.3	Fig. A.4
R/gell3d.R	**R/inverse.R**	**R/conjugate.R**	**R/ellipse-geneig.R**
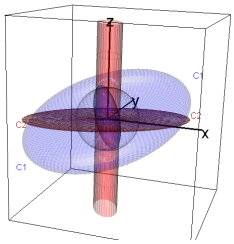	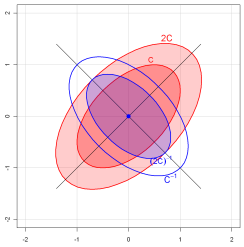	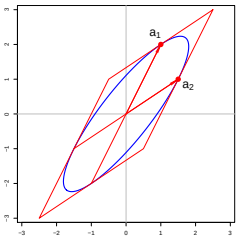	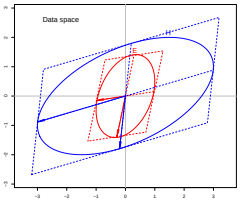

C Movies

Several 3D figures in the paper or this supplementary Apppendix are rendered as static images from different views in the print version. These include Figure 17 and Figure A.1, reproduced below.

These were generated using the **rgl** package in R (Adler and Murdoch, 2011), which allows such 3D views to be rotated, zoomed and otherwise manipulated in 3D space manually, and also supports making animated movies. The movies we created are contained in the `movies/` directory.

References

Adler, D. and Murdoch, D. (2011). *rgl: 3D visualization device system (OpenGL)*. URL `http://CRAN.R-project.org/package=rgl`. R package version 0.92.798.

Dempster, A. P. (1969). *Elements of Continuous Multivariate Analysis*. Reading, MA: Addison-Wesley.

Friendly, M. (2011). *genridge: Generalized ridge trace plots for ridge regression*. URL `http://CRAN.R-project.org/package=genridge`. R package version 0.6-0.

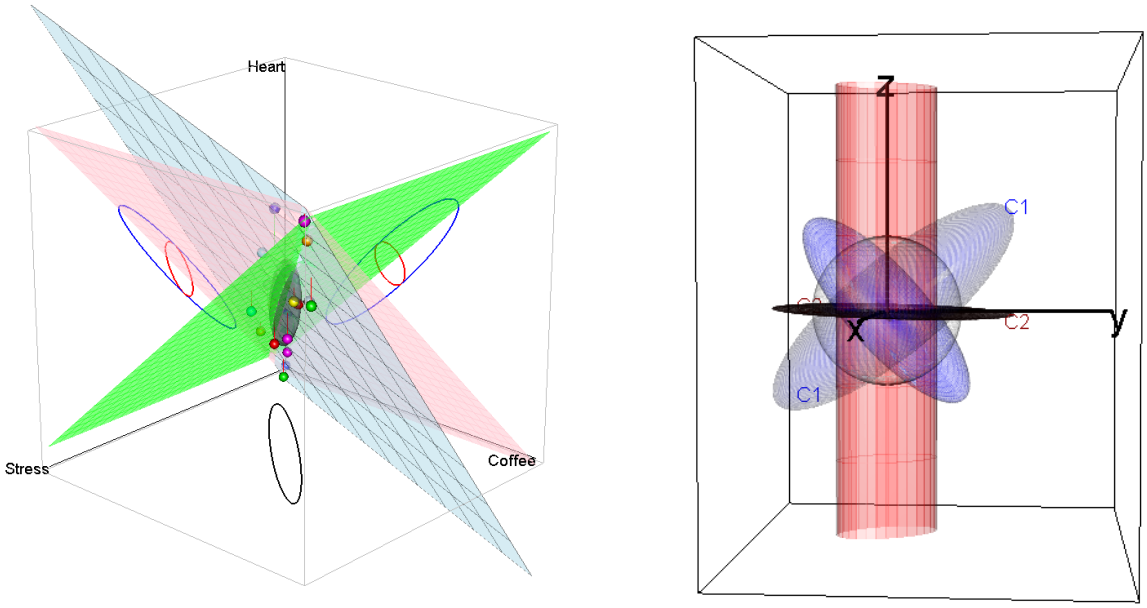

Figure C.1: Left: 3D view of the relationship between Heart, Coffee and Stress, from paper:Figure 17; source: `R/coffee-av3D.R`. Right: 3D view of an example of generalized ellipsoids, from Figure A.1: source: `R/gell3d.R`.

Friendly, M. (2012). The generalized ridge trace plot: Visualizing bias and precision. *Journal of Computational and Graphical Statistics*, 21. URL `http://datavis.ca/papers/genridge.pdf`. In press; Accepted, 2/1/2012.

Monette, G. (2011). *spida: Collection of miscellaneous functions for mixed models etc. prepared for SPIDA 2009*. URL `http://R-Forge.R-project.org/projects/spida/`. R package version 0.1-1/r28.

Monette, G., Friendly, M., and Fox, J. (2011). *p3d: Plot 3d data and fitted surfaces*. URL `http://R-Forge.R-project.org/projects/p3d/`. R package version 0.02-4/r31.